2017

# Identification of Naegleria fowleri proteins linked to primary amoebic meningoencephalitis

Melissa Jamerson
*Virginia Commonwealth University*, hrickomj@vcu.edu

Jacqueline A. Schmoyer
*Virginia Commonwealth University*

Jay Park
*Virginia Commonwealth University*

Francine Marciano-Cabral
*Virginia Commonwealth University*

Guy A. Cabral
*Virginia Commonwealth University*

MICROBIOLOGY

RESEARCH ARTICLE

Jamerson *et al.*, *Microbiology* 2017;163:322–332

DOI 10.1099/mic.0.000428

MICROBIOLOGY SOCIETY

# Identification of *Naegleria fowleri* proteins linked to primary amoebic meningoencephalitis

Melissa Jamerson,[1,2,*] Jacqueline A. Schmoyer,[2] Jay Park,[1] Francine Marciano-Cabral[1] and Guy A. Cabral[1]

**Abstract**

*Naegleria fowleri* (*N. fowleri*) causes primary amoebic meningoencephalitis, a rapidly fatal disease of the central nervous system. *N. fowleri* can exist in cyst, flagellate or amoebic forms, depending on environmental conditions. The amoebic form can invade the brain following introduction into the nasal passages. When applied intranasally to a mouse model, cultured *N. fowleri* amoebae exhibit low virulence. However, upon serial passage in mouse brain, the amoebae acquire a highly virulent state. In the present study, a proteomics approach was applied to the identification of *N. fowleri* amoeba proteins whose expression was associated with the highly virulent state in mice. Mice were inoculated intranasally with axenically cultured amoebae or with mouse-passaged amoebae. Examination by light and electron microscopy revealed no morphological differences. However, mouse-passaged amoebae were more virulent in mice as indicated by exhibiting a two $\log_{10}$ titre decrease in median infective dose 50 ($ID_{50}$). Scatter plot analysis of amoebic lysates revealed a subset of proteins, the expression of which was associated with highly virulent amoebae. MS-MS indicated that this subset contained proteins that shared homology with those linked to cytoskeletal rearrangement and the invasion process. Invasion assays were performed in the presence of a select inhibitor to expand on the findings. The collective results suggest that *N. fowleri* gene products linked to cytoskeletal rearrangement and invasion may be candidate targets in the management of primary amoebic meningoencephalitis.

## INTRODUCTION

*Naegleria fowleri* (*N. fowleri*), depending on environmental conditions, can exist in amoebic, flagellate and cyst forms [1, 2]. *N. fowleri* is ubiquitous in distribution and has been isolated from various freshwater sources, including lakes and ponds [3, 4]. In the free-living amoeba form, it can infect humans and other mammals and can cause a fatal disease known as primary amoebic meningoencephalitis (PAM) [2, 5, 6]. Infection occurs when amoebae enter the nasal passages, attach to the nasal mucosa, pass through the cribriform plate and replicate in the frontal lobes of the brain [2, 7–9]. PAM goes unrecognized generally, and diagnosis, if made, often is prospectively upon autopsy.

*N. fowleri* amoebae maintained axenically (i.e. in culture) are weakly virulent [10–12]. However, when passaged experimentally in mouse brain, they become highly virulent [13, 14]. Studies using mice as experimental hosts have allowed for the identification of factors that putatively promote invasion of the brain, including factors that are attributed to acquisition of the highly virulent state. Collectively, these have suggested that invasion of the brain by amoebae is concentration dependent and occurs in response to host soluble factors emitted from nerve endings located at openings in the cribriform plate [15]. Studies have shown also that *N. fowleri* amoebae emit proteases [16] and elicit a pro-inflammatory response [3] during the invasion process.

Most efforts at preventing human infection with *N. fowleri* have focused on limiting exposure to amoeba-containing water. There are few therapeutic intervention strategies available for limiting spread of the amoebae once infection is initiated. However, it is speculated that amoeba-specified gene products are linked to expansive neuropathology and that these could serve as targets for therapeutic manipulation [17]. In the present investigation, we compared the proteome of axenically cultured, lowly virulent amoebae with that of mouse-passaged, highly virulent amoebae. Each population was indistinguishable microscopically, but mouse-passaged amoebae were over 100-fold more virulent.

Received 29 July 2016; Accepted 11 January 2017

**Author affiliations:** [1]Department of Microbiology and Immunology, Virginia Commonwealth University School of Medicine, Richmond, VA 23298-0678, USA; [2]Department of Clinical Laboratory Sciences, Virginia Commonwealth University School of Allied Health Professions, Richmond, VA 23298-0583, USA.

***Correspondence:** Melissa Jamerson, hrickomj@vcu.edu

**Keywords:** amoeba; mass spectrometry; *N. fowleri*; pathogenicity; primary amoebic meningoencephalitis; proteomics.

**Abbreviations:** CNS, central nervous system; LDH, lactate dehydrogenase; MGF, Mascot generic format; PAM, primary amoebic meningoencephalitis; RT, room temperature.

Assessment of protein fingerprints revealed that mouse-passaged amoebae expressed a subset of proteins associated with cytoskeletal rearrangement and stabilization. One specific protein of interest was identified as having homology with Rho guanine nucleotide exchange factor 28, a protein involved in activation of GTPases of the Rho family, including RhoA. To expand on these observations, invasion assays were performed in the presence of Rhosin, a RhoA inhibitor, and this resulted in a significant decrease in invasion. These results suggest that proteins linked to cytoskeletal rearrangement, stabilization and invasion play a critical role in expansion of neuropathology. These proteins, or associated processes, may serve as targets for therapeutic manipulation.

## METHODS

### Amoebae

*N. fowleri* (ATCC 30894) was obtained from the American Type Culture Collection and grown (37 °C, 24 h) in Oxoid medium [18, 19] in 75 $cm^2$ plastic flasks. Axenically cultured amoebae were maintained (6 months) in this medium to generate weakly virulent *N. fowleri* [10–12]. *N. fowleri* amoebae were passaged (6× at monthly intervals) in male $B_6C_3F_1$ mouse brain following intranasal instillation to generate highly virulent amoebae [14]. For experiments, amoebae were detached from flasks by mechanical bumping and washed (3×) with 0.01 M PBS, pH 7.2.

### Scanning electron microscopy

Amoebae ($2\times10^5$) were placed on coated glass coverslips and fixed (1 h) with 2.5 % glutaraldehyde in 0.1 M cacodylate buffer, pH 7.2. Coverslips then were washed (4×) with PBS, post-fixed (40 min in the dark) with 2 % (w/v) osmium tetroxide buffered in 0.1 M cacodylate buffer, pH 7.2, washed with PBS, dehydrated in a graded series of ethanol, subjected to critical point drying with $CO_2$ as the transitional fluid, mounted on stubs and coated with gold (30 nm) [20]. Samples were examined in a Zeiss EVO 50XVP scanning electron microscope (Zeiss, Oberkochen, Germany) operating at an accelerating voltage of 15 kV.

### Transmission electron microscopy

Amoebae in suspension were transferred to a 15 ml conical tube and pelleted (1000 rcf) in an Eppendorf 5810R centrifuge (Eppendorf North America, Hauppauge, NY). The pellets were fixed in 2.5 % glutaraldehyde buffered with 0.1 M sodium cacodylate (pH 7.2), post-fixed in 2 % osmium tetroxide and processed for transmission electron microscopy [20]. Samples were examined in a JEM 1230 transmission electron microscope (JEOL, Tokyo, Japan) operating at an accelerating voltage of 80 kV.

### Infectious dose

Amoebae ($10^3$–$10^6$ in 20 µl) were introduced intranasally into male $B_6C_3F_1$ mice (5 per group). Mice were monitored up to 7 days for stigmata of infection that included a hunchback, lack of movement, dehydration and loss of weight and ruffled fur. Confirmation of infection was obtained upon recovery of amoebae from cultures of brain explants. The median infective ($ID_{50}$) dose was calculated using the formula:

$ID_{50}$ dose = (% infected at dilution immediately above 50–50 %)/(% infected at dilution immediately above 50 % − % infected at dilution immediately below 50 %).

All procedures in this study were carried out as per the guidelines laid down by the 'Institutional Animal Care and Use Committee' of Virginia Commonwealth University.

### Protein samples

Amoebae were detached from flasks, transferred to 50 ml conical tubes, washed (2×) in PBS and resuspended in lysis buffer (7 M urea, 2 M thiourea, 4 % CHAPS, 30 mM Tris and 5 mM magnesium acetate). An endonuclease (150–300 U, Sigma-Aldrich, St. Louis, MO) inhibitor cocktail and a protease inhibitor cocktail (10 µl, Sigma-Aldrich) were added to each sample. The protein mixture then was incubated (30 min) on ice, sonicated with three 30 s bursts and placed on ice (10 min) after each sonication burst. Samples were centrifuged (10 min, 12 000 ***g***, 4 °C) in an Eppendorf microcentrifuge, transferred to a Spin-X filter microcentrifuge tube (Corning, Corning, NY) and subjected to centrifugation (2 min, 12 000 ***g***, 4 °C). The protein concentration was determined using the RC/DC protein assay (Bio-Rad, Hercules, CA).

### First-dimension isoelectric focusing

A sample volume (50 µg protein) was resuspended in ReadyPrep rehydration/sample buffer (Bio-Rad) to obtain a final volume of 300 µl that was added to a rehydration/sample buffer tray. A 17 cm IPG strip (Bio-Rad, pH range 5–8) was thawed (5 min), placed face down into the sample, overlain with 2 ml mineral oil (Bio-Rad) and allowed to rehydrate overnight at room temperature (RT). Paper wicks (Bio-Rad) were dampened with ultra-pure water and placed at both ends of the focusing tray channel to cover the electrodes. The mineral oil was removed from the rehydrated IPG strip, which then was transferred to the focusing tray channel containing the paper wicks. Mineral oil (2 ml) was pipetted over the IPG strip and the sample was subjected to isoelectric focusing (40 000 volt-hours) using a PROTEAN IEF cell (Bio-Rad). The IPG strips were removed from the focusing tray, the mineral oil was allowed to drain off and the strips were transferred, gel side up, to a clean rehydration/equilibration tray. IPG strips were stored at −80 °C until used for second-dimension electrophoresis.

### Second-dimension electrophoresis

IPG strips were thawed at RT (10–15 min), placed gel side up in a clean rehydration/sample buffer tray and covered with Equilibration Buffer I (Bio-Rad) consisting of 375 mM Tris/HCl, pH 8.8, 6 M urea, 2 % SDS and 2 % DTT. The tray then was subjected to gentle shaking (20 min) using an orbital shaker. Following removal of buffer, the IPG strip was covered with Equilibration Buffer II (Bio-Rad), placed (25 min) on an orbital shaker, dipped in 1× Tris/glycine/

SDS running buffer in a graduated cylinder, placed gel side up onto the back plate of a 10 % SDS-PAGE gel and overlain with agarose. The gel was run at 40 mA per gel until the dye front ran off the bottom of the gel. The gel was then removed from the glass plate and was subjected to Vorum silver staining [21].

### Vorum silver staining

Gels were placed in fixative (50 % MeOH, 12 % acetic acid and 0.05 formalin) overnight at RT, washed (3×) with 35 % ethanol (20 min, RT) and washed twice (10 min each) in ultra-pure deionized water. Gels were sensitized (2 min) with 100 mM sodium thiosulfate (Thermo Fisher Scientific, Waltham, MA) and 30 mM potassium ferricyanide [21] and washed four times (10 min each at RT) with ultra-pure deionized water. Following the last wash, the gels were stained with 0.2 % silver nitrate (AMRESCO, Solon, OH) and 0.076 % formalin (20 min, RT) and rinsed (1 min, 2×) with ultra-pure deionized water. Gels were developed using 6 % sodium carbonate (VWR), 0.05 % formalin and 0.0004 % sodium thiosulfate. The reaction was terminated by washing the gels in stop solution (50 % MeOH and 12 % acetic acid) (20 min, RT) and gels were placed in water (20 min) before scanning using a ScanMaker 9800XL (Microtek, Hsinchu, Taiwan).

### Analysis of 2D gels and liquid chromatography/MS-MS

The scanned 2D gels were analysed using PDQuest ver.8.0.1 differential analysis software (Bio-Rad). Protein identification of in-gel spots was performed by Bioproximity (Chantilly, VA). Briefly, select protein spots were subjected to in-gel digestion (Promega ProteaseMAX in-gel digestion protocol, Promega, Madison, WI) and peptide desalting using C18 stop-and-go extraction tips, and each digestion mixture was analysed by ultra-performance liquid chromatography/MS-MS.

### Data processing and library searching

Mass spectrometer RAW data files were converted to mzML mass spectrometer output file format using msconvert (http://dx.doi.org/10.1038/nbt.2377). Mascot generic format (MGF) files were generated from mzML using the Peak Picker HiRes tool, part of the OpenMS framework (http://dx.doi.org/10.1186/1471-2105-9-163). All searches were performed on Amazon Web Services-based cluster compute instances using the Proteome Cluster interface. MGF files were searched using the most recent protein sequence libraries available from UniProtKB. MGF files were searched using X!!Tandem (http://dx.doi.org/10.1021/pr0701198) using both the native (http://dx.doi.org/10.1093/bioinformatics/bth092) and K-score (http://dx.doi.org/10.1093/bioinformatics/btl379) scoring algorithms and by OMSSA (http://dx.doi.org/10.1021/pr0499491). XML output files were parsed and non-redundant protein sets were determined using Proteome Cluster based on previously published rules (http://dx.doi.org/10.1002/pmic.200900370). MS1-based isotopic features were detected and peptide peak areas were calculated using the FeatureFinder-Centroid tool, part of the OpenMS framework (http://dx.doi.org/10.1186/1471-2105-9-163). Proteins were required to have one or more unique peptides across the analysed samples with E-value scores of 0.0001 or less.

### Invasion assays

Tissue culture inserts (Greiner BioOne, Monroe, NC) with a pore size of 8 µm were coated (50 µl, 30 min, 37 °C) with BD Matrigel (Corning, Corning NY) (5 mg $ml^{-1}$), a reconstituted basement membrane solution which forms a solid matrix. Following the coating period, the inserts were placed in a 24-well tissue culture plate and were used as an upper chamber. Oxoid medium (without serum) was added to the bottom chamber of the tissue culture well to serve as an amoeba attractant. Mouse-passaged *N. fowleri* ($5\times10^4$) suspended in PBS was added to the upper chamber, and the plates were incubated for 24 h at 37 °C. To investigate the functional relevance of RhoA, invasion assays were performed with the addition of Rhosin (a RhoA inhibitor, 30 or 45 µM) (EMD Millipore, Billerica, MA) to the upper chamber. A stock solution of Rhosin was prepared using DMSO. An equal volume of DMSO was added to control inserts, and invasion inhibition was based relative to this control. Additionally, lactate dehydrogenase (LDH) levels were measured using an LDH Cytotoxicity Assay kit (Thermo Scientific) according to the manufacturer's instructions to determine whether Rhosin was toxic to the amoebae at the concentrations used. Amoebae that passed through the Matrigel-coated inserts and into the bottom chamber were counted by video still images (1 $mm^2$) of four random fields using an Olympus CK2 inverted microscope (Opelco, Washington, DC) with an attached XV-GP230 digital video camera (Panasonic, Yokohama, Japan) interfaced to a Dell Dimension XPS1450 computer using Videum 100 hardware and Window NT software (Winnov, Sunnyvale, CA).

### Statistical analysis

Data were expressed as mean±SD of the mean. To determine whether results were statistically significant ($P<0.005$), a two-tailed, unpaired Student's *t*-test was used.

## RESULTS

### Morphology of *N. fowleri* preparations

Axenically cultured and mouse-passaged amoebae were pelleted by centrifugation and the resultant pellets were washed (3×) with PBS and screened for the presence of bacteria by light and scanning electron microscopy. Following the third wash, an aliquot of the wash was used for inoculation of LB medium. No indication of the presence of intracellular bacteria was obtained based on microscopic examination. Similarly, no indication of the presence of viable bacteria was obtained following inoculation of LB medium. Axenically cultured and mouse-passaged amoebae were morphologically indistinguishable based on light and electron microscopy (Fig. 1). Cyst and flagellate forms of *N. fowleri* were absent from both preparations. 'Food cups'

were prominent on both axenically cultured and mouse-passaged amoebae. Similarly, cytoplasmic vacuolar inclusions were prominent within amoebae in both preparations.

### Differential infectious dose of axenically grown versus mouse-passaged *N. fowleri*

The median infective (i.e. $ID_{50}$) dose of axenically cultured and mouse-passaged amoebae was determined. The $ID_{50}$ for axenically cultured amoebae was $3\times10^5$. In contrast, that for mouse-passaged *N. fowleri* was $2\times10^3$, consistent with their being more virulent in the $B_6C_3F_1$ mouse model.

### 2D-PAGE of *N. fowleri* amoeba whole-cell homogenates

*N. fowleri* preparations were screened initially by light microscopy to verify that they were uniformly in the amoeboid state. The protein profile of whole-cell lysates of axenically cultured and mouse-passaged amoebae was then analysed by 2D-PAGE over a pH range of 5–8 and a relative molecular mass ($M^r$) of 10–160 kDa. Following 2D-PAGE, gels were subjected to Vorum silver staining and analysed using PDQuest software. Protein number designations were assigned using the software based on the quadrant sector of the 2D gel in which the spot was located. To control for protein profile variation between repeat gel runs for a specified sample, each sample was assessed three times and the resultant gel profiles were used to create a composite master gel. To control for variation between samples resulting from repeat experiments, separate lots of axenically cultured and mouse-passaged amoebae were evaluated. A representative Gaussian image along with the comparable linear regression computation for a composite master gel of three replicate gels from an individual analysis is shown in Fig. 2. Regression analysis indicated a correlation coefficient greater than 0.9, consistent with reproducibility of protein profiles. Scatter plot analysis of master gels demonstrated that protein spots detected for either axenically cultured or mouse-passaged amoebae were each within a two fold range of the linear regression line, coincident with a one-to-one correspondence line intersecting the X–Y axis. Using scatter plot analysis, three sets of protein spots were identified. Protein spots for which levels were identified as exceeding 2 SD from the best-fit line plotting mouse-passaged versus axenically cultured amoebae were designated as having a 95 % likelihood of being linked to the mouse-passaged state. Protein spots for which levels were identified at 2 SD below the best-fit line were designated as having a 95 % likelihood of being associated with axenically cultured amoebae. Protein spots for which levels were identified as being within 2 SD of the best-fit line were attributed as being associated with both mouse-passaged and axenically cultured amoebae.

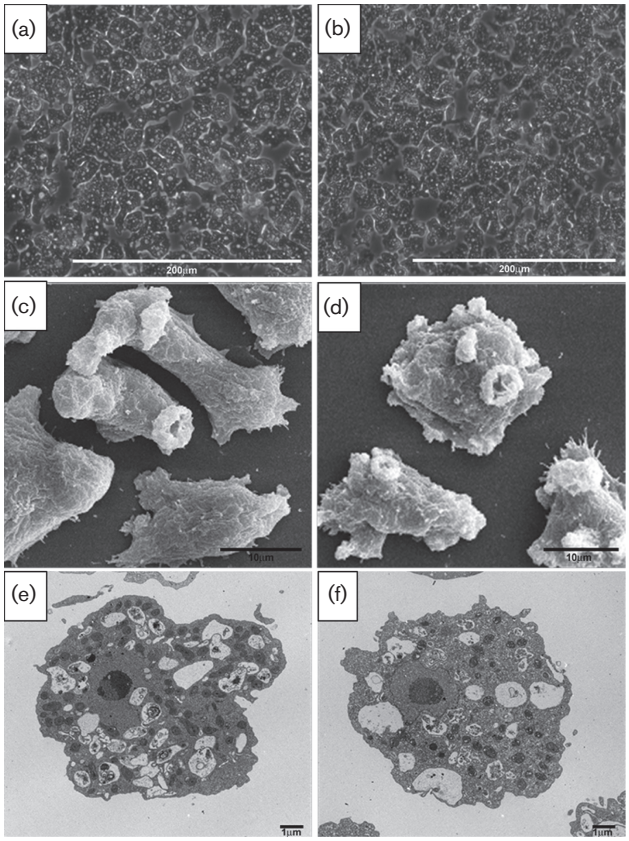


**Fig. 1.** Comparative microscopic assessment of axenically cultured versus mouse-passaged amoebae. No morphologic difference was observed between axenically grown and mouse-passaged amoebae. (a, b) Light microscopy; (c, d) scanning electron microscopy; (e, f) transmission electron microscopy.

### Axenically cultured and mouse-passaged *N. fowleri* exhibit a differential protein profile

The protein fingerprint generated from master gels for axenically grown and mouse-passaged *N. fowleri* was distinctive (Fig. 3). Linear regression analysis demonstrated a correlation coefficient between mouse-passaged and axenically cultured protein spots of 0.69, consistent with a pattern of differential protein expression. Based on scatter plot assessment of master gels, three populations of protein spots were identified. A subset of 12 protein spots was found to be associated with whole-cell homogenates of mouse-passaged amoebae, a subset of 14 protein spots was associated with whole-cell homogenates of axenically cultured amoebae and an excess of 120 protein spots were identified as common in whole-cell homogenates of mouse-passaged and axenically cultured amoebae.

### Analysis of protein spots associated with whole-cell homogenates of mouse-passaged amoebae

A subset of 6 of 12 protein spots that was found to be associated with whole-cell homogenates of mouse-passaged amoebae was subjected to further analysis (Fig. 4). These were selected based on their prominence upon Vorum staining. Gaussian representation on bar graphs of these six protein spots (Fig. 5, middle lane) was assigned a standard spot (SSP) number by the PDQuest software. The selected protein spots varied in relative molecular mass from 30 to 65 kDa. These were excised and processed for MS-MS and data were analysed by three algorithms (X!Tandem, OMSSA and K-score)

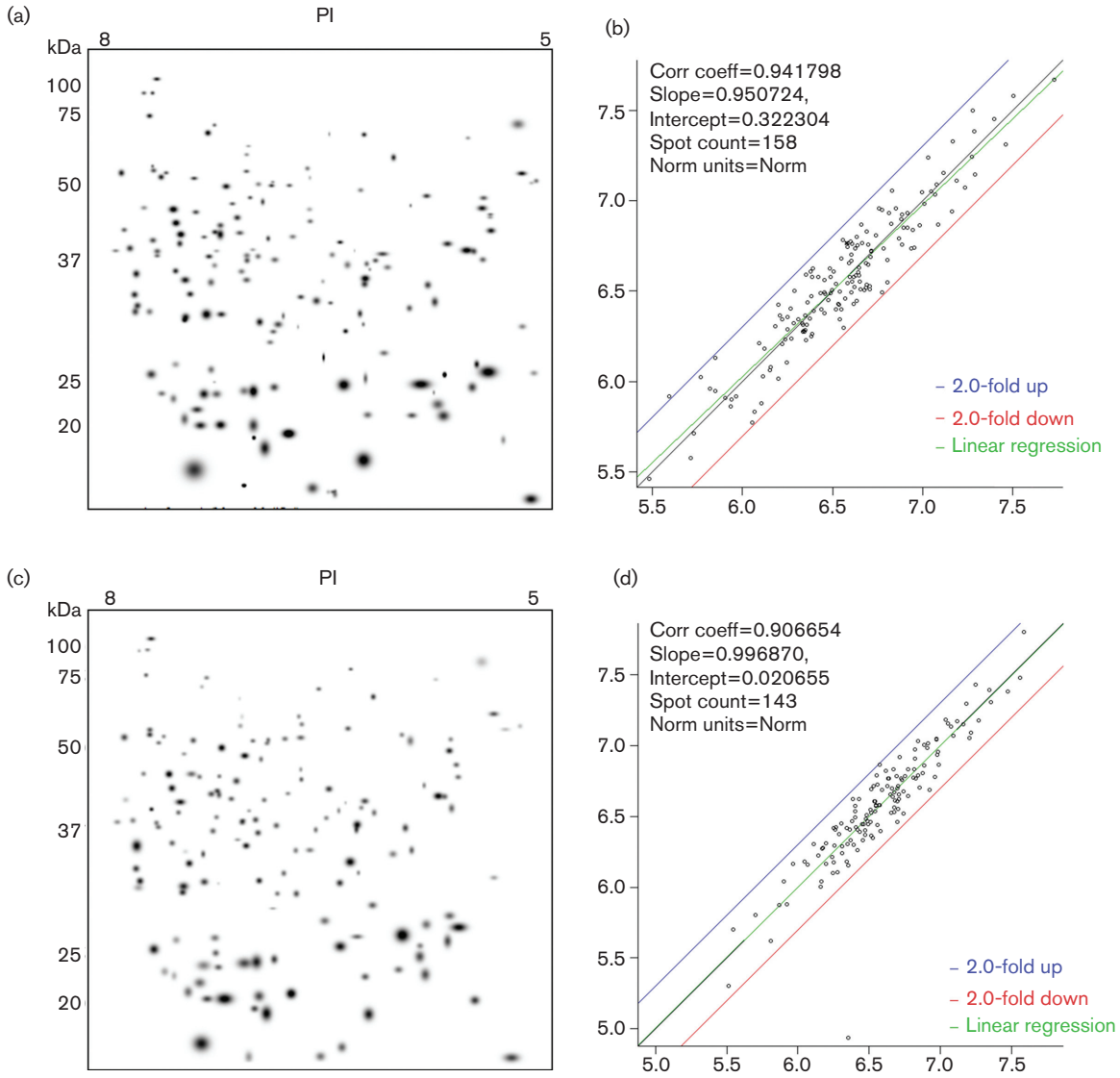


**Fig. 2.** Representative Gaussian image and comparable linear regression computation for a composite master gel for mouse-passaged (a, b) versus axenically grown (c, d) amebae.

for homology of known proteins. Results of these analyses are summarized in Table 1. Proteins were identified as having homology to structural and signalling proteins, including those involved in downstream signalling of integrins. Included among these (spot 1507) was Rho guanine nucleotide exchange factor 28 that functions as a RhoA-specific guanine nucleotide exchange factor regulating signalling pathways downstream of integrin and growth factor receptors.

## RhoA inhibition using Rhosin treatment reduces amoebae invasion

In order to establish a functional linkage between the identified signalling proteins and PAM pathology, invasion assays were performed in the presence of Rhosin, a RhoA inhibitor. Highly virulent *N. fowleri* was added to Matrigel-coated tissue culture inserts in the presence of Rhosin (30 or 45 µM in PBS) or vehicle drug control (DMSO in PBS) at the same time as the lower chambers were loaded with Oxoid medium (serum-free). Amoebae that were exposed to 30 µM Rhosin had no significant decrease in invasion compared to the non-treated control (Fig. 6b, d). However, the amoebae treated with 45 µM Rhosin demonstrated a significant decrease in invasion (Fig. 6c, d, $P<0.005$). The percentage inhibition was calculated and determined to be approximately 11 % when amoebae were treated with 30 µM Rhosin compared to 65 % inhibition when treated with 45 µM Rhosin (Fig. 6e). To ensure that the inhibition was not due to cytotoxic effects of the drug, LDH assays were performed. All treatments used were shown to be non-toxic to the amoebae (data not shown).

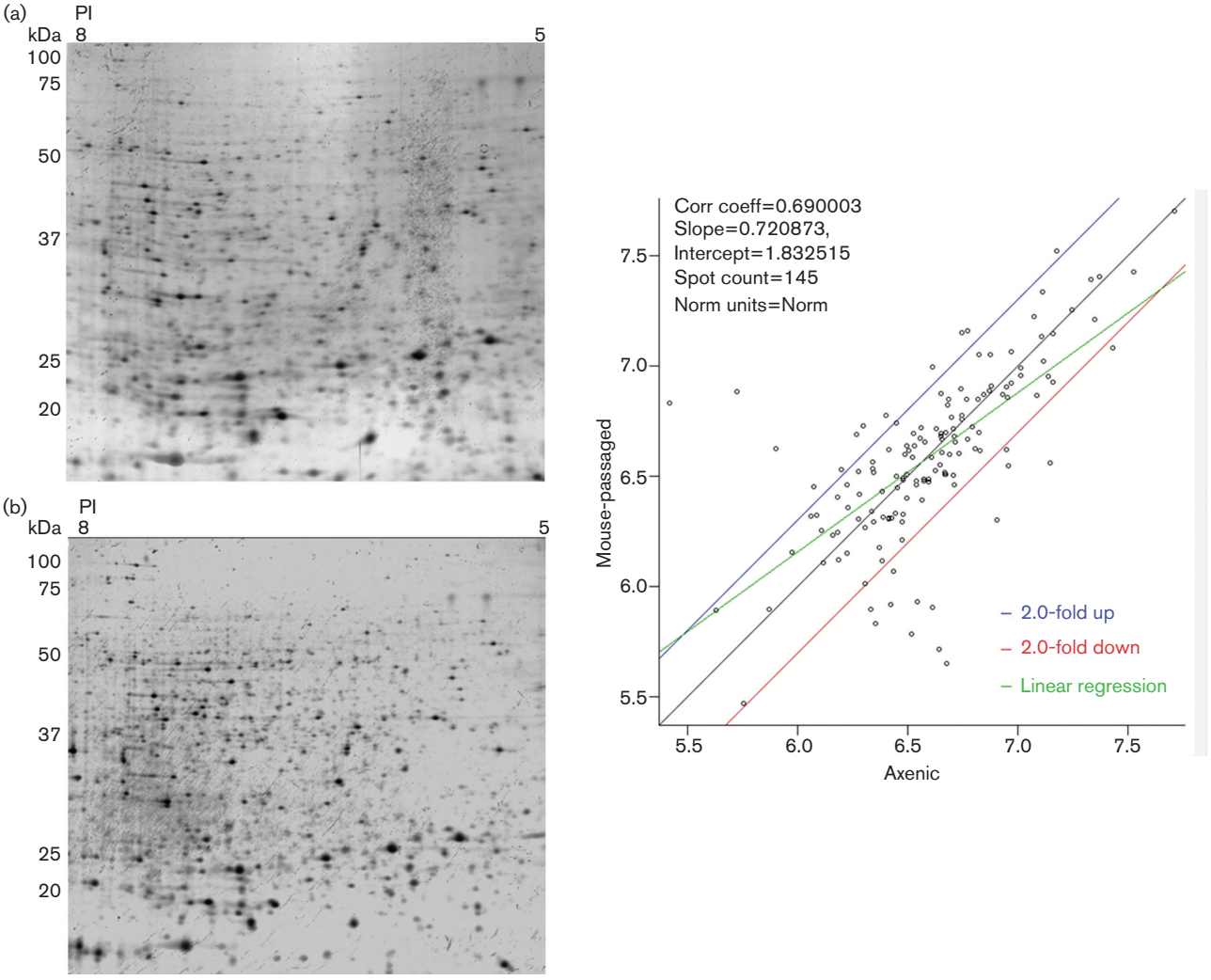


**Fig. 3.** The protein fingerprint generated from master gels for axenically grown (a) and mouse-passaged (b) *N. fowleri* is distinctive. Linear regression analysis (right panel) demonstrated a correlation coefficient between mouse-passaged and axenically grown amoebae proteins of 0.69, consistent with a pattern of differential protein expression.

## DISCUSSION

PAM is a complex disease that, in its earliest stages, involves attachment of amoebae to nasal epithelium followed by their passage through into the brain via the nasal mucosa. It has been suggested that the attachment process results in activation of *N. fowleri* signal transduction pathways leading to the production and release of mucosal layer-eroding proteases [16]. *N. fowleri* harbours a membrane protein related to the human integrin-like receptor [22] and a fibronectin-binding protein essential for the interaction of trophozoites with extracellular matrix glycoproteins [23]. Reveiller *et al.* [24] isolated a membrane protein from pathogenic *N. fowleri*, designated Mp2CL5, that was not found in non-pathogenic *Naegleria* species. The investigators implicated this protein as playing a role in pathogenicity. Zysset-Burri *et al.* [25] found that this protein was expressed at higher levels in highly virulent amoeba trophozoites as compared to weakly virulent trophozoites. However, while various gene products have been implicated in virulence, an *N. fowleri*-specified gene product that is expressed early in central nervous system (CNS) infection and that could serve as a candidate therapeutic target to limit expansion of PAM has yet to be identified.

In the present investigation, microscopic examination revealed no identifiable morphological differences between axenically cultured and mouse-passaged *N. fowleri* amoebae. Both populations of amoebae displayed ‘food cups’ or amoebastomes. These structures have been linked to the ingestion of bacteria by *N. fowleri* amoebae when found free in the environment [26], and to the ingestion of nerve cells [27]. Nevertheless, in spite of morphological similarity, axenically cultured and mouse-passaged *N. fowleri* amoebae

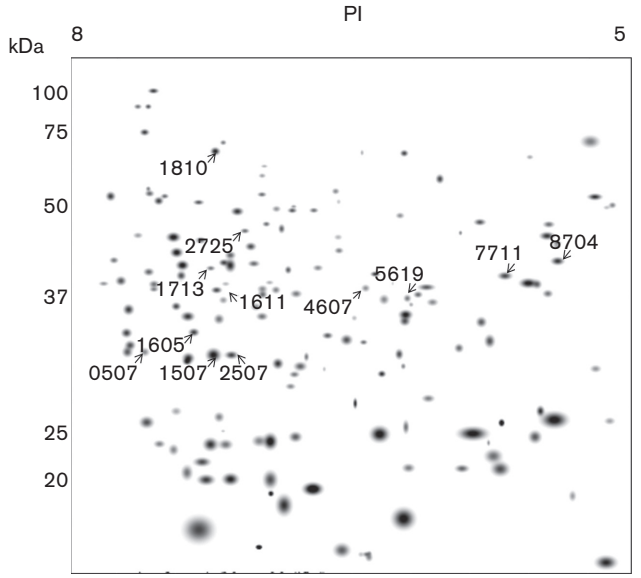


**Fig. 4.** Protein spots from the Master Gel Profile of whole-cell homogenates shown to be associated with mouse-passaged amoebae. These were given a standard spot (SSP) number automatically assigned by the PDQuest software. Spots in the lower left region of the image have low SSP numbers, while spots in the upper right region have high SSP numbers. The first two digits of a spot's SSP number correspond to its section's X and Y coordinates. Spots within a section are numbered sequentially.

were distinctive in their virulence when used to infect mice. Mouse-passaged amoebae were more lethal in that a 100-fold less concentration was required to exert 50 % mortality following their intranasal introduction.

In order to address whether newly synthesized or hyperproduced *N. fowleri*-specified proteins were associated with expansive neuropathogenesis, analytical 2D-PAGE in concert with MS was performed. All *N. fowleri* preparations were screened initially by light and electron microscopy to verify that they consisted of trophozoites. Whole-cell lyates of *N. fowleri* amoebae were processed for 2D-PAGE and analysed using the PDQuest software. Spots on 2D gels were plotted in terms of their relation to two SD values from a one-to-one correspondence of a best-fit line that compared the protein profile of mouse-passaged versus axenically grown amoebae. Subpopulations of proteins were identified as having a 95 % likelihood of association with the mouse-passaged state, a 95 % likelihood of association with axenically cultured amoebae or a 95 % likelihood of association with both mouse-passaged and axenically cultured amoebae. However, these three subpopulations were identified only within the context of a 2D gel for which the isoelectric points ranged from pH 5 to pH 8 and relative molecular masses ranged from 10 to 160 kDa. Thus, amoeba-specified proteins having highly basic and highly acidic properties or a relative molecular mass less than 10 kDa were excluded from analysis. Nevertheless, within the defined parameters, the collective observations suggest that mouse-passaged amoebae undergo a 'reconstruction' of protein profiles upon acquisition of the highly virulent state. The majority of protein spots were identified within two SD values of the best-fit regression line and probably represent proteins common to mouse-passaged and axenically cultured amoebae. A second set of protein spots was identified at two SD values below the best-fit regression line and probably represent proteins whose expression is requisite to amoebae when found free in the environment. The third set of protein spots for which levels were identified as exceeding two SD values from the best-fit regression line of mouse-passaged versus axenically cultured amoebae probably represents proteins that are associated with the *N. fowleri* amoebae when in the highly virulent state.

Six protein spots from this third set were selected for further analysis by liquid chromatography/MS-MS. The peptide databases were searched for closely homologous, but not identical, sequences. Included among these was a protein spot that was identified as having a sequence comparable to that of Rho guanine nucleotide exchange factor 28 protein. Rho guanine nucleotide exchange factors are involved in activating GTPases in the Rho family, including RhoA. RhoA is prevalent in the cytoplasm and, among other functional attributes, regulates signalling pathways downstream of integrin and growth factor receptors [28]. It is involved in the formation of focal adhesions and cell motility [28], and plays a functionally relevant role in activities associated with early stages of CNS infection such as effector cell target cell attachment and invasion [29, 30]. Adhesion to the extracellular matrix is mediated by focal adhesions, specialized regions of the plasma membrane. At these focal contacts, bundles of actin filaments are anchored to transmembrane receptors of the integrin family through a multimolecular complex of junctional plaque proteins [28]. It has been reported that RhoA and Rho-kinase activation promotes the development of cancer, leaving patients more susceptible to cancer metastasis, specifically by regulation of the actin cytoskeleton. It has been suggested, also, that inhibition of RhoA and Rho-kinase reduces tumour burden and facilitates termination of the proliferative response of a variety of cancers [31, 32].

Previously, we have shown that *N. fowleri* exhibits focal adhesion-like structures when attached to extracellular matrix components [22]. Additionally, MS analysis has detected a Rho family small GTPase present in *N. fowleri* isolates [33]. Since inhibitors of RhoA and Rho-kinases suppress the expansion and migration of cancer cells, we postulated that these may have a comparable effect on *N. fowleri* amoebae. Therefore, to provide functional data in support of the MS observations, invasion assays were performed in the presence or absence of Rhosin, a specific Rho inhibitor. Indeed, invasion assays in the presence of Rhosin (45 μM) had a significantly lower number of amoebae that were able to invade the Matrigel-coated inserts, further providing evidence that RhoA plays a functional role in the *N. fowleri*

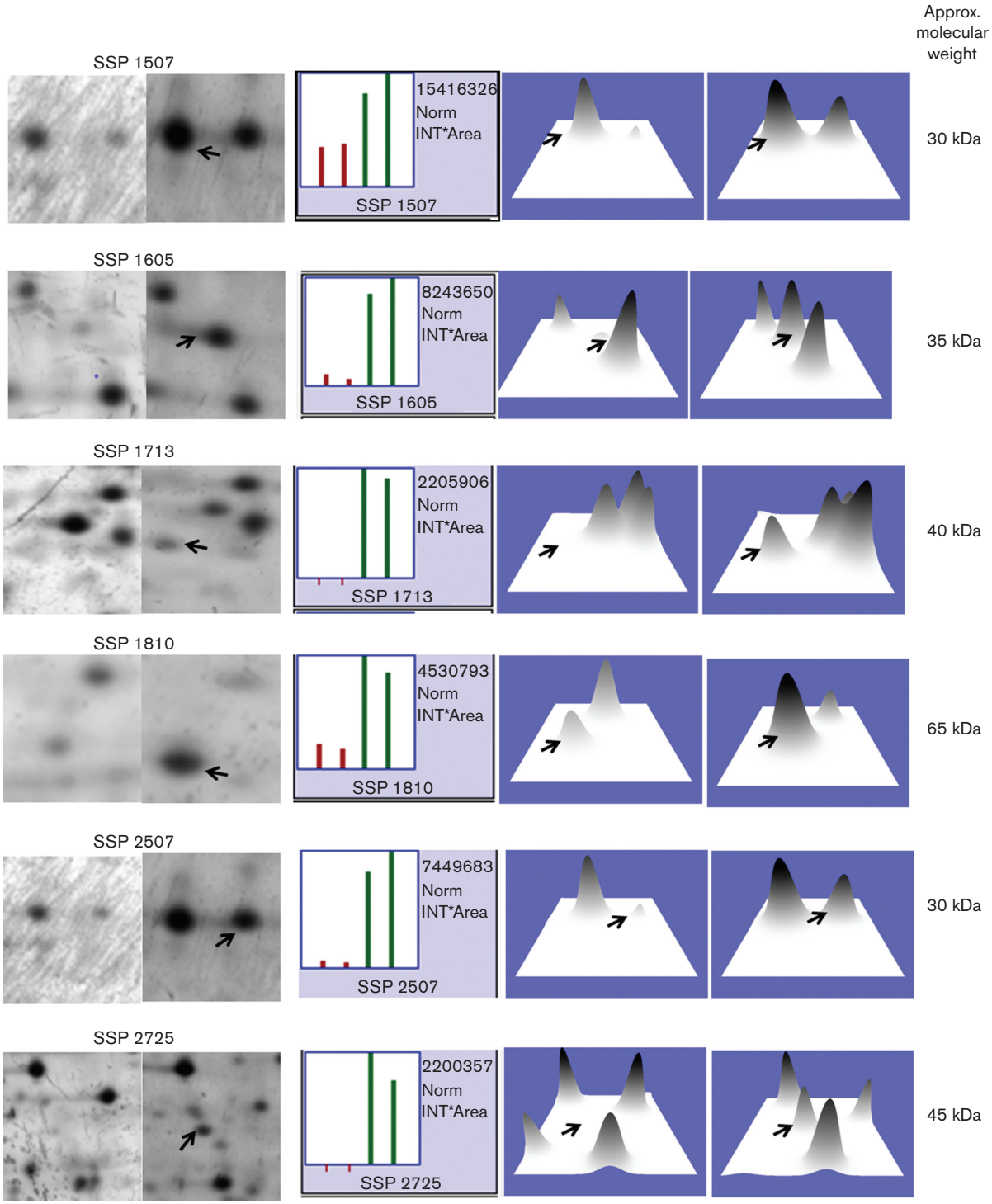


**Fig. 5.** Protein spots from the Master Gel Profile of whole-cell homogenates shown to be associated with mouse-passaged amoebae were selected for analysis by MS. Gaussian representation on bar graphs (middle lane) of these six protein spots (left lane) from duplicate master gels indicated their reproducibility.

invasion process. Rho-signalling pathways have been shown to play a role in the invasive nature of other amoebae, including *Entamoeba histolytica* [29].

While the mechanism by which differential gene expression promotes PAM in the CNS remains to be defined, it is possible that exposure to exogenous or host-specified

**Table 1.** Ultra-performance liquid chromatography MS-MS analysis

Data were analysed by three MS-MS protein algorithms (X!Tandem, OMSSA and K-score) for homology to known proteins.

| Spot number | Peptide | Protein name | Gene name | Description |
|---|---|---|---|---|
| 1507 | RELAEVPASIPVNTRYLNLQENSIQVIR | D3Z2D1 | Lrrc4b | Leucine-rich repeat containing protein 4B |
| | LKESLPR | Q8C3×4 | Guf1 | Translation factor Guf1, mitochondrial |
| | | P97433 | Arhgef28 | Rho guanine nucleotide exchange factor 28 |
| | AVFPSIVGRPR | Q3UAA9 | Actb | Putative uncharacterized protein (actb) |
| | TVPPAVPGVTFLSGGQSEEEASLNLNAINR | P05063 | Aldoc | Fructose-biphosphate aldolase C |
| | FGANAILGVSLAVCK | B0QZL1 | Eno 1 | Enolase |
| | LSSSTEQSTSSRLVR | P51141 | Dv11 | Segment polarity protein dishevelled homologue DVL1 |
| | FTASAGIQVVGDDLTVTNPKR | Q5FW97 | EG433182 | Enolase I, alpha non-neuron |
| | LHFFMPGFAPLTSR | Q8WUC1 | Tubb5 | Tubulin beta-5 chain |
| | RFDEILEASDGIMVAR | Q91Y18 | Pkm | Pyruvate kinase PKM |
| | AYHEQLSVAEITNACFEPANQMVK | Q5XJF8 | Tuba1a | Tubulin alpha-1A chain |
| | LAVEALSSLDGDLSGR | Q04447 | Ckb | Creatine kinase B-type |
| 1605 | LKESLPR | Q8C3×4 | Guf1 | Translation factor Guf1, mitochondrial |
| | TVPPAVPGVTFLSGGQSEEEASLNLNAINR | P05063 | Aldoc | Fructose-biphosphate aldolase C |
| | FGANAILGVSLAVCK | B0QZL1 | Eno1 | Enolase |
| | AVFPSIVGRPR | Q3UAA9 | Actb | Putative uncharacterized protein (actb) |
| | AVGLVIPSLNGK | Q94625 | | Peptide with no match |
| | MSDGLFLECCR | D2VQ70 | | Peptide with no match |
| | FPHELVSSTAIEGVRDSSFDVIHK | D2V7S3 | | Peptide with no match |
| | MSDGLFLECCR | D2VQ70 | | Peptide with no match |
| 1713 | TVPPAVPGVTFLSGGQSEEEASLNLNAINR | P05063 | Aldoc | Fructose-biphosphate aldolase C |
| | FGANAILGVSLAVCK | B0QZL1 | Eno1 | Enolase |
| | AVFPSIVGRPR | Q3YAA9 | Actb | Putative uncharacterized protein (actb) |
| | FPHELVSSTAIEGVRPDSSFDVIHK | D2V7S3 | | Peptide with no match |
| 1810 | LSSSTEQSTSSRLVR | P51141 | Dvl1 | Segment polarity protein dishevelled homologue DVL1 |
| | AVFPSIVGRPR | Q3UAA9 | Actb | Putative uncharacterized protein (actb) |
| 2507 | LKESLPR | Q8C3×4 | Guf1 | Translation factor Guf1, mitochondrial |
| | TVPPAVPGVTFLSGGQSEEEASLNLNAINR | P05063 | Aldoc | Fructose-biphosphate aldolase C |
| | FGANAILGVSLAVCK | B0QZL1 | Eno1 | Enolase |
| | LSSTEQSTSSRLVR | P51141 | Dvl1 | Segment polarity protein dishevelled homologue |
| | RFDEILEASDGIMVAR | Q91YI8 | Pkm | Pyruvate kinase PKM |
| | LAVEALSSLDGDLSGR | Q04447 | Ckb | Creatine kinase B-type |
| | KEVEVFKSEEALGLTITDNGAGYAFIK | Q9Z0G0 | Gipc1 | PDZ domain-containing protein GIPC1 |
| | AVFPSIVGRPR | Q3UAA9 | Actb | Putative uncharacterized protein (actb) |
| 2725 | DIQMTQTPSSLSASLGDRVSISCR | P01649 | | Ig kappa chain V-V regions |
| | KLDLEGIGRPTVPEFRTPKGK | P56931 | E2F2 | Transcription factor E2F2 |
| | TRLQESSQQKR | Q8R2M2 | Dnttip2 | Deoxynucleotidyltransferase terminal-interacting protein 2 |

components serves to promote differential gene expression by the amoebae. For example, Hu *et al.* [34] examined protein synthesis patterns of a weakly virulent *N. fowleri* LEE strain from axenic culture, the same strain after mouse passage and the same strain after growth on bacteria. Numerous changes in protein synthesis were attributed to the transformation of the LEE strain from low to high virulence. These investigators concluded that some changes in protein synthesis could be linked directly to virulence. Recently, Zysset-Burri *et al.* [25] conducted an intra-species comparison of *N. fowleri* amoebae based on the model proposed by Burri *et al.* [35]. They indicated that trophozoites maintained in Nelson's medium or PYNFH medium supplemented with liver hydrolysate (LH, PYNFH/LH medium) were highly virulent in mice. They also demonstrated their rapid proliferation *in vitro*. In contrast, trophozoites cultured in PYNFH medium were weakly virulent and exhibited slower growth. Heat shock protein 70, actin 1 and 2, the membrane protein Mp2CL5 and cyclophilin were identified at increased levels in highly virulent trophozoites. A 1D electrophoresis in concert with nano-liquid chromatography/MS-MS revealed a total of 2166 proteins, 477 of which were expressed differentially between weakly virulent trophozoites maintained in PYNFH medium and highly virulent trophozoites in PYNFH/LH medium. Among the 43 proteins that were co-regulated in highly virulent *N. fowleri*

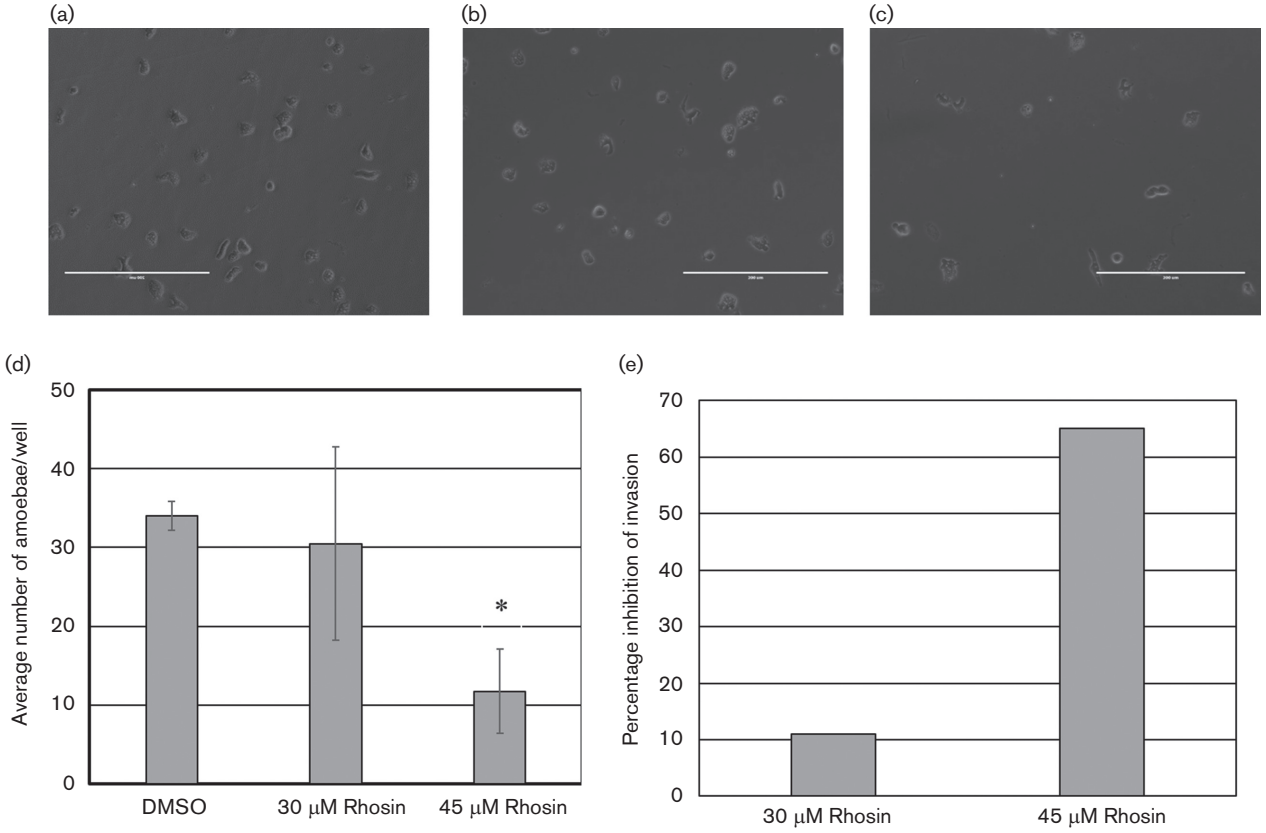


**Fig. 6.** Rhosin treatment decreases highly virulent *N. fowleri* invasion through Matrigel. Light micrographs depicting highly virulent *N. fowleri* that invaded to the bottom of the chamber in the presence of (a) vehicle control, (b) 30 μM Rhosin and (c) 45 μM Rhosin. Amoebae were counted (average number per well) and percentage inhibition was determined (d and e). Experiments were performed in triplicate. The vertical bars in Fig. 6(d) represent SD while the asterisk represents $P<0.005$ by Student's *t*-test.

populations, 22 were up-regulated and were considered to represent putative pathogenicity factors. Zysset-Burri *et al.* [25] demonstrated also that when the PYNFH medium was supplemented with LH, *N. fowleri* trophozoites converted to the highly virulent phenotype. Clustering of newly identified potential pathogenicity factors from *N. fowleri* according to their gene ontology affiliations suggested that they localized at the cellular membrane, in cellular vesicles or at cell projections. These observations led the investigators to conclude that the membrane was a key location where pathogenic processes most likely occurred and that these involved actin-dependent vesicular trafficking.

In summary, the published collective data suggest that *N. fowleri* amoeba attachment to host cell components constitutes a key event in the early infectivity process. Such attachment may activate signal transductional pathways that culminate in triggering differential expression in which a subset of proteins promotes invasion and proliferation of *N. fowleri* amoebae within the CNS. PAM often goes unrecognized and effective therapeutic intervention has yet to be realized. Identification of target points in the amoebic replicative cycles that could limit expansive proliferation within the CNS offers an attractive option for limiting PAM, particularly since the disease is often diagnosed after the onset of clinical symptoms. Studies are in progress to further assess the functional relevance of these candidate proteins as potential therapeutic targets for limiting expansive PAM.

Funding information
This work was supported in part by the 2016 Virginia Commonwealth University Presidential Research Quest Fund (PeRQ Fund).

Conflicts of interest
The authors declare that there are no conflicts of interest.

Ethical statement
All procedures in this study were carried out as per the guidelines laid down by the 'Institutional Animal Care and Use Committee' of Virginia Commonwealth University.

References

1. Carter RF. Description of a *Naegleria* sp. isolated from two cases of primary amoebic meningo-encephalitis, and of the experimental pathological changes induced by it. *J Pathol* 1970;100:217–244.
2. Martinez AJ. *Free-Living Amoebas: Natural History, Prevention, Diagnosis, Pathology, and Treatment of Disease*. Boca Raton, FL: CRC Press; 1985.

3. Marciano-Cabral F, Cabral GA. The immune response to *Naegleria fowleri* amebae and pathogenesis of infection. *FEMS Immunol Med Microbiol* 2007;51:243–259.
4. Martinez AJ, Visvesvara GS. Free-living, amphizoic and opportunistic amebas. *Brain Pathol* 1997;7:583–598.
5. Carter RF. Primary amoebic meningo-encephalitis: clinical, pathological and epidemiological features of six fatal cases. *J Pathol Bacteriol* 1968;96:1–25.
6. Cerva L, Novăk K. Amoebic meningoencephalitis: 16 fatalities. *Science* 1968;160:92.
7. Carter RF. Primary amoebic meningo-encephalitis. An appraisal of present knowledge. *Trans R Soc Trop Med Hyg* 1972;66:193–213.
8. Jarolim KL, Mccosh JK, Howard MJ, John DT. A light microscopy study of the migration of *Naegleria fowleri* from the nasal submucosa to the central nervous system during the early stage of primary amebic meningoencephalitis in mice. *J Parasitol* 2000;86:50–55.
9. Martinez J, Duma RJ, Nelson EC, Moretta FL. Experimental *Naegleria meningoencephalitis* in mice. Penetration of the olfactory mucosal epithelium by *Naegleria* and pathologic changes produced: a light and electron microscope study. *Lab Invest* 1973;29:121–133.
10. Marciano-Cabral F, Toney DM. Modulation of biological functions of *Naegleria fowleri* amoebae by growth medium. *J Eukaryot Microbiol* 1994;41:38–46.
11. Whiteman LY, Marciano-Cabral F. Susceptibility of pathogenic and nonpathogenic *Naegleria* spp. to complement-mediated lysis. *Infect Immun* 1987;55:2442–2447.
12. Wong MM, Karr SL Jr, Chow CK. Changes in the virulence of *Naegleria fowleri* maintained *in vitro*. *J Parasitol* 1977;63:872–878.
13. Bradley SG, Toney DM, Zhang Y, Marciano-Cabral F. Dependence of growth, metabolic expression, and pathogenicity of *Naegleria fowleri* on exogenous porphyrins. *J Parasitol* 1996;82:763–768.
14. Toney DM, Marciano-Cabral F. Alterations in protein expression and complement resistance of pathogenic *Naegleria* amoebae. *Infect Immun* 1992;60:2784–2790.
15. Brinkley C, Marciano-Cabral F. A method for assessing the migratory response of *Naegleria fowleri* utilizing [$^3$H]uridine-labeled amoebae. *J Protozool* 1992;39:297–303.
16. Vyas IK, Jamerson M, Cabral GA, Marciano-Cabral F. Identification of peptidases in highly pathogenic vs. weakly pathogenic *Naegleria fowleri* amebae. *J Eukaryot Microbiol* 2015;62:51–59.
17. Grace E, Asbill S, Virga K. *Naegleria fowleri*: pathogenesis, diagnosis, and treatment options. *Antimicrob Agents Chemother* 2015;59:6677–6681.
18. Band RN, Balamuth W. Hemin replaces serum as a growth requirement for *Naegleria*. *Appl Microbiol* 1974;28:64–65.
19. Cline M, Marciano-Cabral F, Bradley SG. Comparison of *Naegleria fowleri* and *Naegleria gruberi* cultivated in the same nutrient medium. *J Protozool* 1983;30:387–391.
20. Pettit DA, Williamson J, Cabral GA, Marciano-Cabral F. *In vitro* destruction of nerve cell cultures by *Acanthamoeba* spp.: a transmission and scanning electron microscopy study. *J Parasitol* 1996;82:769–777.
21. Vorum H, Østergaard M, Hensechke P, Enghild JJ, Riazati M *et al.* Proteomic analysis of hyperoxia-induced responses in the human choriocarcinoma cell line JEG-3. *Proteomics* 2004;4:861–867.
22. Jamerson M, da Rocha-Azevedo B, Cabral GA, Marciano-Cabral F. Pathogenic *Naegleria fowleri* and non-pathogenic *Naegleria lovaniensis* exhibit differential adhesion to, and invasion of, extracellular matrix proteins. *Microbiology* 2012;158:791–803.
23. Han KL, Lee HJ, Shin MH, Shin HJ, Im KI *et al.* The involvement of an integrin-like protein and protein kinase C in amoebic adhesion to fibronectin and amoebic cytotoxicity. *Parasitol Res* 2004;94:53–60.
24. Réveiller FL, Suh SJ, Sullivan K, Cabanes PA, Marciano-Cabral F. Isolation of a unique membrane protein from *Naegleria fowleri*. *J Eukaryot Microbiol* 2001;48:676–682.
25. Zysset-Burri DC, Müller N, Beuret C, Heller M, Schürch N *et al.* Genome-wide identification of pathogenicity factors of the free-living amoeba *Naegleria fowleri*. *BMC Genomics* 2014;15:496.
26. Marciano-Cabral F. Biology of *Naegleria spp*. *Microbiol Rev* 1988;52:114–133.
27. Marciano-Cabral FM, Fulford DE. Cytopathology of pathogenic and nonpathogenic *Naegleria* species for cultured rat neuroblastoma cells. *Appl Environ Microbiol* 1986;51:1133–1137.
28. Marjoram RJ, Lessey EC, Burridge K. Regulation of RhoA activity by adhesion molecules and mechanotransduction. *Curr Mol Med* 2014;14:199–208.
29. Franco-Barraza J, Zamudio-Meza H, Franco E, Del Carmen Domínguez-Robles M, Villegas-Sepúlveda N *et al.* Rho signaling in *Entamoeba histolytica* modulates actomyosin-dependent activities stimulated during invasive behavior. *Cell Motil Cytoskeleton* 2006;63:117–131.
30. Kim JC, Crary B, Chang YC, Kwon-Chung KJ, Kim KJ. *Cryptococcus neoformans* activates RhoGTPase proteins followed by protein kinase C, focal adhesion kinase, and ezrin to promote traversal across the blood-brain barrier. *J Biol Chem* 2012;287:36147–36157.
31. Abe H, Kamai T, Hayashi K, Anzai N, Shirataki H *et al.* The Rho-kinase inhibitor HA-1077 suppresses proliferation/migration and induces apoptosis of urothelial cancer cells. *BMC Cancer* 2014;14:412.
32. Pillé JY, Denoyelle C, Varet J, Bertrand JR, Soria J *et al.* Anti-RhoA and anti-RhoC siRNAs inhibit the proliferation and invasiveness of MDA-MB-231 breast cancer cells *in vitro* and *in vivo*. *Mol Ther* 2005;11:267–274.
33. Moura H, Izquierdo F, Woolfitt AR, Wagner G, Pinto T *et al.* Detection of biomarkers of pathogenic *Naegleria fowleri* through mass spectrometry and proteomics. *J Eukaryot Microbiol* 2015;62:12–20.
34. Hu WN, Band RN, Kopachik WJ. Virulence-related protein synthesis in *Naegleria fowleri*. *Infect Immun* 1991;59:4278–4282.
35. Burri DC, Gottstein B, Zumkehr B, Hemphill A, Schürch N *et al.* Development of a high- versus low-pathogenicity model of the free-living amoeba *Naegleria fowleri*. *Microbiology* 2012;158:2652–2660.


Edited by: V. J. Cid